Spatiotemporal Summation and Recognition Effects for a Dual-Emitter Light-Induced Neuromorphic Device

Yongchao Yang, Zheng Shi, Bingcheng Zhu, Jialei Yuan, Guixia Zhu, Xumin Gao, Yuanhang Li, Zhiyu Zhang, Yuhuai Liu, and Yongjin Wang

***Abstract*— We propose and fabricate a dual-emitter light-induced neuromorphic device composed of two light-induced devices with a common collector and base. Two InGaN multiple-quantum-well diodes (MQW-diodes) are used as the emitters to generate light, and one InGaN MQW-diode is used as the common collector to absorb the emitted light. When the presynaptic voltages are synchronously applied to the two emitters, the collector demonstrates an adding together of the excitatory postsynaptic voltage (EPSV). The width and period of the two input signals constitute the code to generate spatial summation and recognition effects at the same time. Experimental results confirm that temporal summation caused by the repetitive-pulse facilitation could significantly strengthen the spatial summation effect due to the adding together behavior when the repetitive stimulations are applied to the two emitters in rapid succession. Particularly, the resonant summation effect occurs at the cosummation region when the two repetitive-pulse signals have a resonant period, which offers a more sophisticated spatiotemporal EPSV summation function for the dual-emitter neuromorphic device.**

***Index Terms*— Adding together behavior, dual-emitter light-induced neuromorphic device, excitatory postsynaptic voltage (EPSV), InGaN multiple-quantum-well diodes (MQW-diodes), resonant summation effect (RSE).**

I. Introduction

THE artificial synaptic device is a hot topic for brain-inspired neuromorphic systems [1]–[7], and synaptic electronics have gained considerable attention in recent years, including two-terminal memristors and three-terminal ionic/electronic hybrid devices. Based on phase change materials, nanoelectronic programmable synapses have been developed for brain-inspired computing [8]. Dynamic logic and learning have been presented using a carbon nanotube synapse [9]. An Ag_2S inorganic synapse has been reported to emulate the synaptic functions of both short-term plasticity and long-term potentiation characteristics [10]. Flexible metal oxide/grapheme oxide hybrid neuromorphic devices have demonstrated the realization of spatiotemporal correlated logics [11]. Proton-conducting grapheme oxide-coupled neuron devices have been proposed for brain-inspired cognitive systems [12]. The number of optic nerve fibers is enormous in the eyes. When we see an object, the information is carried along the optic nerves in the eyes to the brain and thus, the brain interprets what we see. It is an extremely complicated communication, which are analogous to the communication system consisting of a transmitter and receiver. Compared with other synaptic devices, the light-induced synaptic device uses photons rather than electrons or protons to induce excitatory postsynaptic voltage (EPSV) behavior for artificial synapse applications. EPSV summation represents the simplest form of synaptic communication. An enormous number of neurons can perform more sophisticated computations, requiring that many EPSVs add together to produce a significant postsynaptic summation. Therefore, the light-induced artificial synapse with multiple inputs is a preferred choice for the emulation of optic nerves, which are essential to sense light stimulations in the eyes. In addition, light-induced artificial synapse can work with dual operation modes, providing a promising approach to develop complicated artificial neurons and to perform sophisticated neural computation [13].

Here, we propose and fabricate a dual-emitter light-induced neuromorphic device on an III-nitride-on-silicon platform. Nerve impulses are mimicked in the light-induced artificial synapses, and we focus on the development of artificial synapse network with multiple presynapses. Fig. 1 shows a schematic illustration of the proposed dual-emitter light-induced neuromorphic device, which has a common base (B). The collector (C) absorbs the pulse light generated by the emitter (E) to achieve a photon–electron conversion, leading to an EPSV for the mimicking of synaptic activity with different

Manuscript received October 30, 2017; accepted November 18, 2017. Date of publication December 4, 2017; date of current version December 27, 2017. This work was supported in part by the National Science Foundation of China under Grant 61322112 and Grant 61531166004, in part by the Special Project under Grant 2016YFE0118400, and in part by the Natural Science Foundation of Jiangsu Province under Grant BE2016186. The review of this paper was arranged by Editor M. M. Cahay. *(Corresponding author: Yongjin Wang.)*

Y. Yang, Z. Shi, B. Zhu, J. Yuan, G. Zhu, X. Gao, Y. Li, and Y. Wang are with the Grünberg Research Center, Nanjing University of Posts and Telecommunications, Nanjing 210003, China (e-mail: wangyj@njupt.edu.cn).

Z. Zhang is with the Changchun Institute of Optics, Fine Mechanics and Physics, Chinese Academy of Science, Changchun 130033, China.

Y. Liu is with the Department of Electronics Engineering, Zhengzhou University, Zhengzhou 450001, China.

Color versions of one or more of the figures in this paper are available online at http://ieeexplore.ieee.org.

Digital Object Identifier 10.1109/TED.2017.2776969

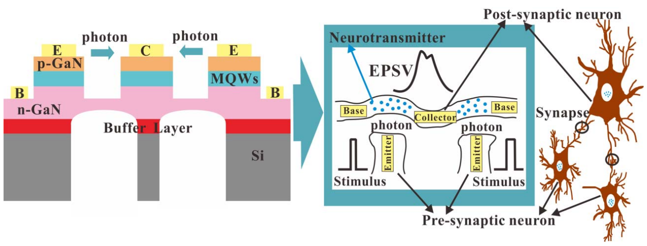

Fig. 1. Schematic of a dual-emitter neuromorphic device.

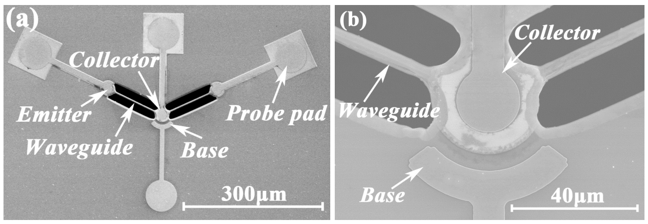

Fig. 2. (a) SEM image of fabricated dual-emitter neuromorphic device. (b) High-magnification image of the collector and base.

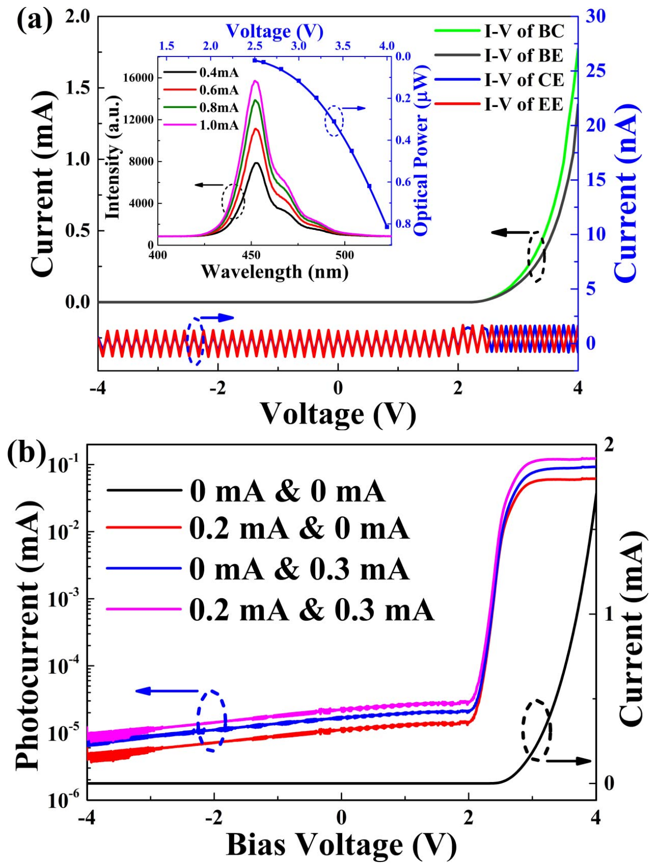

Fig. 3. (a) I–V curves of the dual device, and the inset is EL spectra and optical power of the emitter. (b) Induced collector photocurrent versus forward current of the emitter.

signal sources. The period, shape, and width of pulses constitute the code to transfer information in the biological nervous system, which is characterized by the EPSV summation [14]. When the two emitters are synchronously biased, the EPSVs happen at the same time and are added together, leading to a spatial summation. The adding together of EPSVs generated at the same emitter forms a temporal summation if they occur in a rapid succession. The spatial summation can be significantly reinforced by the temporal summation, which is investigated for emulating the complicated memory effect during the learning process.

II. Experimental Results and Discussion

The dual-emitter neuromorphic device is implemented on a 2-in III-nitride-on-silicon wafer. The top GaN-based epitaxial films are grown on silicon substrate by metalorganic chemical vapor deposition. The 1500-μm-thick starting wafer is first thinned to approximately 200 μm by chemical–mechanical polishing. The emitter, collector, and probing pad are patterned by photolithography and formed by induced coupled plasma reactive ion etching (ICP-RIE) of III-nitride epitaxial films with Cl_2 and BCl_3 hybrid gases at the flow rates of 10 and 25 sccm, respectively. The Ni/Au (20 nm/180 nm) metal stacks are used as p- and n-type contacts. Then, waveguide structures are defined and etched by ICP-RIE. After protecting the top device structure with thick photoresist, silicon removal is conducted by deep reactive ion etching with alternating steps of SF_6 etching and C_4F_8/O_2 passivation. Subsequently, III-nitride backside thinning is carried out by ICP-RIE to obtain ultrathin membrane-type device architecture. Fig. 2(a) shows a scanning electron microscope (SEM) image of the fabricated dual-emitter neuromorphic device, which is a four-terminal device. The suspended device architecture can form a highly confined waveguide structure for the in-plane light coupling between the emitter and the collector. Two InGaN multiple-quantum-well diodes (MQW-diodes) are used as the emitters to generate light and one InGaN MQW-diode serves as a common collector to absorb the in-plane-guided light through suspended waveguides. The two emitters are connected to the collector via two 100-μm-long, 2.47-μm high, and 6-μm-wide suspended waveguides, and the electrodes are connected to the 70-μm-diameter probe pads for device characterization. A 10-μm-wide isolation gap is used between the collector and the common base, as illustrated in Fig. 2(b).

Fig. 3(a) summarizes the current–voltage (I–V) curves of the dual-emitter device, which are characterized by an Agilent B1500A semiconductor device analyzer. The base contact is probably 150 μm away from emitter contact, and there will be a large resistance in BE. Hence, the I–V curve of BE shows a relatively small current. According to the I–V curve of EE, the electrical isolation is obtained, indirectly indicating that the signal is coupled optically. The inset of Fig. 3(a) shows the measured electroluminescence (EL) spectra of single light emitter at different injection currents, which are measured using an Ocean Optics USB4000 spectrometer. The light emission intensity depends on the injection current, and the dominant emission wavelength locates around 452 nm. The optical output power from single light emitter is controlled by the injection current of the MQW-emitter. The I–V curve of BC exhibits a typical rectifying behavior without light absorption, which is used to normalize the induced photocurrent with light absorption. The collector absorbs the emitted light to generate

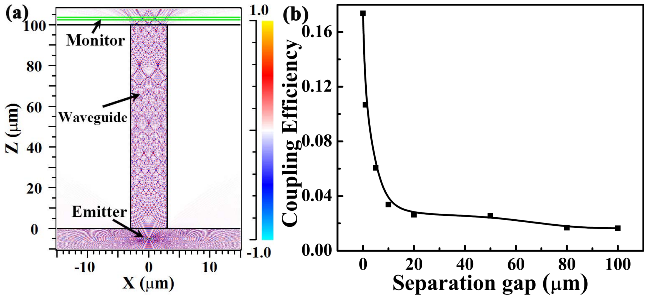

Fig. 4. (a) Light coupling without separation gap. (b) Coupling efficiency as a function of separation gap.

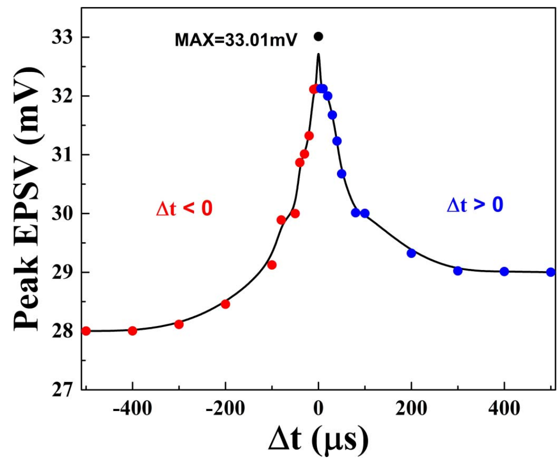

Fig. 5. STDP performance.

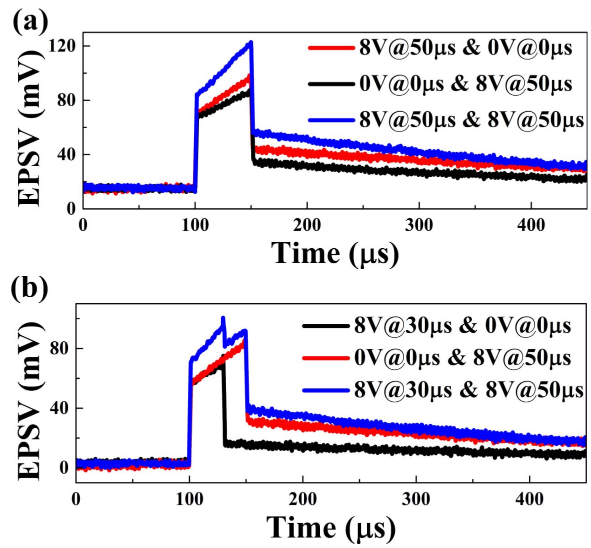

Fig. 6. Spatial EPSV summation. (a) Same width. (b) Different widths.

the photocurrent. When the two emitters are separately driven by the injection currents of 0 and 0.2 mA to emit light, Fig. 3(b) shows an increased photocurrent with increasing bias voltage of the collector from −4 to 4 V, in which the collector exhibits two light detection modes. Because the two emitters are symmetrical, an increased photocurrent is observed when the two emitters are synchronously driven by the injection currents of 0.3 and 0 mA. The light intensity is modulated by the injection current of the emitter, so the induced photocurrent is dependent on the injection current of the emitter. Thus, the generated photons from different emitters can be accumulated when both emitters are operating simultaneously. The induced photocurrent is added together when both emitters simultaneously operate with the injection currents of 0.3 and 0.2 mA.

Fig. 4(a) shows the calculated light coupling between the emitter and the collector through suspended waveguide at a wavelength of 452 nm using beam propagation simulation, in which the refractive index of waveguide used is 2.45 and suspended waveguide is 100-μm long and 6-μm wide. Assuming that the suspended waveguide has a separation gap in the middle, Fig. 4(b) shows the calculated coupling efficiency as a function of the separation gap. The coupling efficiency is significantly decreased with increasing the separation gap from 0 to 100 μm, indicating that the light being coupled in the waveguide does play a dominant role in the light coupling between the emitter and the collector because these optical components are fabricated on the same membrane [15].

This paper begins with the spatial EPSV summation of the collector that operates under the light detection mode. Signal coupling between presynaptic signals is time dependent, leading to the spike-time-dependent plasticity (STDP) behavior [16]. We measured the STDP performance of two signals arriving at different moments. As shown in Fig. 5, the coupling of two signals arriving at the same time would obtain maximum spatial summation. Therefore, we focus on the simultaneous spatiotemporal summation, in which activation from two presynaptic devices turns out at the same time.

Fig. 6(a) shows the spatial summation of the collector, in which two 8 V at 50 μs pulse signals are separately applied to the two emitters at the same time. Both the collector and the base operate at zero bias, and the two emitters are biased at 2.4 V. Compared to the EPSV generated by a single pulse signal from one emitter, the integrated EPSV amplitude increases, and the decay time extends, leading to an improved spatial summation effect. Moreover, the adding together of EPSVs is dependent on the pulse widths, as illustrated in Fig. 6(b). One 8 V at 50-μs pulse signal and one 8 V at 30-μs pulse signal are synchronously applied to the two emitters. The EPSV is integrated when two emitters are operating. The EPSV is then abruptly dropped and gradually increases when one pulse signal is terminated and only one emitter is driven by another pulse signal. Finally, the EPSV amplitude gradually returns toward its initial state due to the decay behavior when the later pulse signal is also ended. The EPSV summation can enhance the signal amplitudes and remain their differences, and the integrated EPSVs can be decoded into simple signals that distinctly identify the light source, leading to a recognition function. The dual-emitter device can achieve signal recognition through a spatial EPSV summation process when the signal pulse widths are different.

Repetitive-pulse facilitation (RPF) behavior occurs when the stimulation is continuously applied. Many EPSVs add together to produce a temporally integrated EPSV and finally reach a saturated value, which is determined by the initial

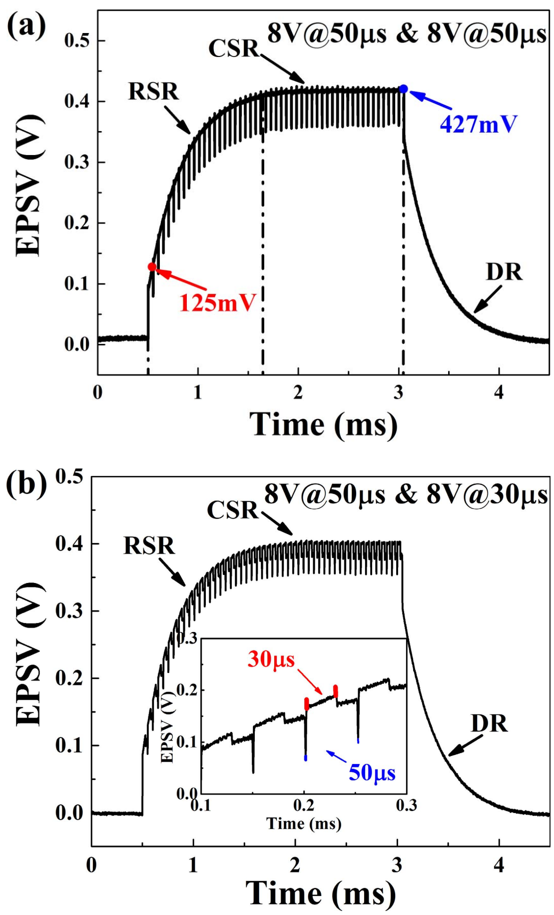

Fig. 7. Spatiotemporal summation under (a) same pulse widths and (b) different pulse widths.

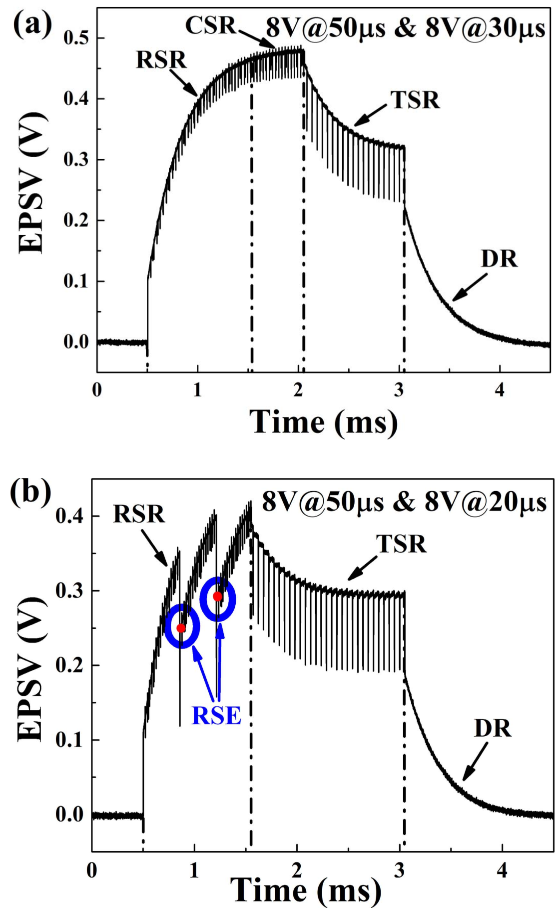

Fig. 8. Spatiotemporal summation behavior under (a) same signal period and (b) different signal periods.

amplitude of the pulse signal. However, it is still difficult to obtain a high temporal EPSV summation for the desired integration effect even if weak pulse signals are continuously applied [17]. To address this issue, the improved temporal EPSV behavior could be achieved through an adding together of spatial EPSV summation in a dual-emitter light-induced neuromorphic device. Two repetitive 8 V at 50 μs pulse signals are separately applied to the two emitters simultaneously, in which the pulse number is 50 with the same pulse interval of 1 μs. Fig. 7(a) shows that the integrated EPSV amplitude increases and is eventually saturated as the pulse number increases. Compared to the first integrated EPSV amplitude of 125 mV, the saturated EPSV value is significantly increased to 427 mV. The 8 V at 50 μs pulse signal has a pulse interval of 1 μs, the 8 V at 30 μs pulse signal has a pulse interval of 21 μs, and the pulse numbers are 50. Fig. 7(b) illustrates that the EPSV integration effect is improved due to the adding together of temporal and spatial summation and signal recognition can simultaneously be obtained when repetitive stimulations with different pulse widths happen at the same period.

The spatiotemporal summation for a dual-emitter light-induced device is highly sensitive to the period of the repetitive-pulse signals. Compared to the spatial summation of two single signals from two emitters, the spatiotemporal summation behavior can be divided into a rapid summation region (RSR), a cosummation region (CSR), a temporal summation region (TSR), and a decay region, as shown in Fig. 8(a). The pulse numbers of two repetitive signals are 50. One signal has a pulsewidth of 50 μs and a pulse interval of 1 μs, and the other has pulsewidth of 30 μs and a pulse interval of 1 μs, corresponding to the signal periods of 51 and 31 μs, respectively. Two RPF behavior patterns occur at RSR, and the integrated EPSV amplitude is quickly increased. As the pulse number increases, the integrated EPSV amplitude enters into the CSR, in which the difference between the two signals leads to the signal recognition at a high EPSV level. When one repetitive signal is ended, the cosummation effect is stopped and the saturated EPSV amplitude is quickly dropped and enters into the TSR, in which only one RPF takes place. When the later signals are finished, the EPSV gradually returns to the initial state, resulting in a decay process. When the numbers of the two repetitive-pulse signals are increased, a periodic EPSV summation occurs, which relates to the resonant period. Fig. 8(b) shows that sophisticated summation function occurs when the two repetitive-pulse signals have a resonant period in the cosummation process. The two repetitive signals have the signal periods of 51 and 21 μs, respectively. Therefore, the two repetitive-pulse signals have a resonant period of 357 μs, leading to a distinct resonant summation effect (RSE). Taken together, it can be concluded that the RSE provides a more complicated summation function for a multiple-emitter device, resulting in the simultaneous summation and recognition of multiple signals at a high level.

III. Conclusion

In conclusion, we propose and fabricate a dual-emitter light-induced neuromorphic device to investigate the adding together of temporal and spatial EPSV summation effect. The integrated EPSV behavior occurs when pulse signals are synchronously applied to the two emitters. The period and width of signals lead to improved summation and recognition behavior at the same time. Experimental results confirm that the summation effect could be significantly strengthened due to the adding together of EPSV summation when repetitive stimulations are applied to the two emitters. Particularly, the RSE occurs at the CSR when the two repetitive-pulse signals have a resonant period, which provides a more sophisticated spatiotemporal EPSV summation function.

References

[1] S. Song, K. D. Miller, and L. F. Abbott, "Competitive Hebbian learning through spike-timing-dependent synaptic plasticity," *Nature Neurosci.*, vol. 3, pp. 919–926, Sep. 2000, doi: 10.1038/78829.

[2] L. F. Abbott and W. G. Regehr, "Synaptic computation," *Nature*, vol. 431, pp. 796–803, Oct. 2004, doi: 10.1038/nature03010.

[3] L. Q. Zhu, C. J. Wan, L. Q. Guo, Y. Shi, and Q. Wan, "Artificial synapse network on inorganic proton conductor for neuromorphic systems," *Nature Commun.*, vol. 5, Jan. 2014, Art. no. 3158, doi: 10.1038/ncomms4158.

[4] Q. Lai, L. Zhang, Z. Li, W. F. Stickle, R. S. Williams, and Y. Chen, "Ionic/electronic hybrid materials integrated in a synaptic transistor with signal processing and learning functions," *Adv. Mater.*, vol. 22, pp. 2448–2453, May 2010, doi: 10.1002/adma.201000282.

[5] X. Yang *et al.*, "Nonassociative learning implementation by a single memristor-based multi-terminal synaptic device," *Nanoscale*, vol. 8, pp. 18897–18904, Aug. 2016, doi: 10.1039/C6NR04142F.

[6] F. Alibart *et al.*, "An organic nanoparticle transistor behaving as a biological spiking synapse," *Adv. Funct. Mater.*, vol. 20, no. 2, pp. 330–337, Jan. 2010, doi: 10.1002/adfm.200901335.

[7] C.-H. Kim, S. J. Sung, and M.-H. Yoon, "Synaptic organic transistors with a vacuum-deposited charge-trapping nanosheet," *Sci. Rep.*, vol. 6, Sep. 2016, Art. no. 33355, doi: 10.1038/srep33355.

[8] D. Kuzum, R. G. D. Jeyasingh, B. Lee, and H.-S. P. Wong, "Nanoelectronic programmable synapses based on phase change materials for brain-inspired computing," *Nano Lett.*, vol. 12, no. 5, pp. 2179–2186, Jun. 2011, doi: 10.1021/nl201040y.

[9] K. Kim, C.-L. Chen, Q. Truong, A. M. Shen, and Y. Chen, "A carbon nanotube synapse with dynamic logic and learning," *Adv. Mater.*, vol. 25, no. 12, pp. 1693–1698, 2013, doi: 10.1002/adma.201370080.

[10] T. Ohno, T. Hasegawa, T. Tsuruoka, K. Terabe, J. K. Gimzewski, and M. Aono, "Short-term plasticity and long-term potentiation mimicked in single inorganic synapses," *Nature Mater.*, vol. 10, pp. 591–595, Aug. 2011, doi: 10.1038/nmat3054.

[11] C. J. Wan *et al.*, "Flexible metal oxide/graphene oxide hybrid neuromorphic transistors on flexible conducting graphene substrates," *Adv. Mater.*, vol. 28, no. 28, pp. 5878–5885, 2016, doi: 10.1002/adma.201600820.

[12] C. J. Wan *et al.*, "Proton-conducting graphene oxide-coupled neuron transistors for brain-inspired cognitive systems," *Adv. Mater.*, vol. 28, no. 18, pp. 3557–3563, 2016, doi: 10.1002/adma.201505898.

[13] Y. H. Li *et al.*, "Light induced synaptic transistor with dual operation modes," *IEEE Electron Device Lett.*, vol. 37, no. 11, pp. 1434–1437, Nov. 2016, doi: 10.1109/LED.2016.2607998.

[14] M. F. Bear, B. W. Connors, and M. A. Paradiso, *Neuroscience: Exploring the Brain*, 3rd ed. London, U.K.: Williams & Nargate, 2006.

[15] Y. Yang, J. Yuan, Y. Li, X. Gao, and Y. Wang, "On-chip integration for in-plane video transmission using visible light," *Proc. SPIE, Optoelectron. Devices Integr. VI*, vol. 10019, p. 1001912, Oct. 2016, doi: 10.1117/12.2247728.

[16] H. Tian *et al.*, "Graphene dynamic synapse with modulatable plasticity," *Nano Lett.*, vol. 15, no. 12, pp. 8013–8019, Oct. 2015, doi: 10.1021/acs.nanolett.5b03283.

[17] G. X. Zhu *et al.*, "Saturation behavior for a comb-like light-induced synaptic transistor," *IEEE Electron Device Lett.*, vol. 38, no. 1, pp. 71–74, Jan. 2017, doi: 10.1109/LED.2016.2627044.

Yongchao Yang was born in Yizheng, Jiangsu, China, in 1992. He is currently pursuing the M.S. degree with the Nanjing University of Posts and Telecommunications, Nanjing, China.

His current research interests include the light-emitting diodes and photodiodes and its application in visible light communication.

Zheng Shi received the B.Sc. and Ph.D. degrees from the Nanjing University of posts and telecommunications, Nanjing, China, in 2010 and 2016, respectively.

He is currently an Assistant Professor. He is also a Professor with the Nanjing University of Posts and Telecommunications. His current research interests include InGaN/Gan LED design and fabrication for visible light communication applications.

Bingcheng Zhu received the Ph.D. degree in information and communication engineering from Southeast University, Nanjing, China, in 2015.

He was a Visiting Student with The University of British Columbia, Kelowna, BC, Canada, in 2014. His current research interests include free-space optical communications, visible light communications, diversity over fading channels, and cooperative communications.

Jialei Yuan was born in Suzhou, Jiangsu, China, in 1993. He received the B.S. degree in electronic information engineering from Nanjing Normal University, Nanjing, China, in 2015. He is currently pursuing the M.S. degree with the Nanjing University of Posts and Telecommunications, Nanjing.

His current research interests include design and fabrication of devices.

Guixia Zhu was born in Taizhou, Jiangsu, China, in 1992. She received the B.S. degree in electronic and computer engineering from the Nanjing University of Posts and Telecommunications, Nanjing, China, where she is currently pursuing the M.S. degree.

Her current research interests include behaviors for a synaptic transistor by using photon instead of electron or proton, light-emitting diodes, and photodiodes.

Xumin Gao was born in Lu'an, Anhui, China, in 1991. She is currently pursuing the Ph.D. degree with the Nanjing University of Posts and Telecommunications, Nanjing, China.

Her current research interests include the light-emitting diodes and its application in visible light communication.

Yuanhang Li was born in Suzhou, Anhui, China, in 1993. He is currently pursuing the bachelor's degree from the Nanjing University of Posts and Telecommunications, Nanjing, China.

His current research interests include visible light communication device testing and system construction.

Zhiyu Zhang is currently an Associate Professor with the Changchun Institute of Optics, Fine Mechanics and Physics, Chinese Academy of Sciences, Changchun, China. His current research interests include ultraprecision machining, laser direct writing, micro-/nanomanufacturing, and laser processing for optical fabrication.

Yuhuai Liu received the Ph.D. degree from the Anhui Institute of Optics and Fine Mechanics, Chinese Academy of Sciences (CAS), Hefei, China, in 1999.

He was with the Institute of Semiconductors, CAS, Beijing, China, The University of Tokushima, Tokushima, Japan, Mie University, Tsu, Japan, and Tohoku University, Sendai, Japan, till 2011, a Professor with Zhengzhou University, Zhengzhou, China, and a Visiting Professor with Nagoya University, Nagoya, Japan.

Yongjin Wang received the Ph.D. degree from the Shanghai Institute of Microsystem and Information Technology, Chinese Academy of Sciences, Shanghai, China, in 2005.

He is currently a Professor with the Nanjing University of Posts and Telecommunications, Nanjing, China. His current research interests include nitride semiconductors, visible light communications as well as artificial synaptic devices.